Received: 16 September 2018 | Revised: 3 November 2018 | Accepted: 11 November 2018
DOI: 10.1002/ardp.201800275

FULL PAPER

DPhG ARCH PHARM
Archiv der Pharmazie

Novel acyl thiourea derivatives: Synthesis, antifungal activity, gene toxicity, drug-like and molecular docking screening

Lyudmyla Antypenko[1] | Fatuma Meyer[1] | Olena Kholodniak[2] | Zhanar Sadykova[1] | Tereza Jirásková[1] | Anastasiia Troianova[1] | Vladlena Buhaiova[1] | Surui Cao[1] | Sergiy Kovalenko[2] | Leif-Alexander Garbe[1] | Karl G. Steffens[1]

[1] Faculty of Agriculture and Food Science, Neubrandenburg University, Neubrandenburg, Germany

[2] Department of Organic and Bioorganic Chemistry, Zaporizhzhya State Medical University, Zaporizhzhya, Ukraine

Correspondence
Lyudmyla Antypenko, Department of Food and Bioproduct Technology, Neubrandenburg University, Brodaer Str. 2, 17033 Neubrandenburg, Germany.
Email: antypenkol@gmail.com

Funding information
Enamine Ltd.; German Federal Ministry of Education and Research, Grant number: FKZ 03FH025IX4

Abstract

Nine novel acyl thioureas were synthesized. Their identities and purities were confirmed by LC-MS spectra; each structure was elucidated by elemental analysis, IR, ^{1}H and ^{13}C NMR spectra. Applying an *in vitro* screening of their antifungal potential, three substances (**3**, **5**, and **6**) could be selected as showing high activity against 11 fungi and 3 *Phytophthora* strains of phytopathogenic significance. Analysis of gene toxicity with the *Salmonella* reverse mutagenicity test, as an assessment of drug likeness, lipophilicity, and calculations of frontier molecular orbitals assign a low toxicity profile to these compounds. Molecular docking studies point to 14α-demethylase (CYP51) and *N*-myristoyltransferase (NMT) as possible fungal targets for growth inhibition. The findings are discussed with respect to structure–activity relationship (SAR).

KEYWORDS
anti-phytopathogens, drug likeness, gene toxicity, molecular docking, *N*-(2-carbamothioylhydrazine-1-carbonothioyl)cyclopropanecarboxamide, *N*-substituted *N*-(hydrazinecarbonothioyl)-cyclopropanecarbox(benz)amides

1 | INTRODUCTION

Substances with antifungal activity are of eminent importance in human health care, veterinary medicine, and agriculture. Low toxicity and environmental friendliness are further mandatory properties making such chemicals ready for commercialization. Unfortunately, the occurrence of fungal strains resistant toward standard antifungals has developed to an extent threatening established treatment regimens against fungal infections and food security for a growing world population.[1] Therefore, the search for novel, potent biologically active compounds is an ongoing need to cope with challenges caused by the emergence of new resistant fungi. In this context derivatives based on thiourea core warrant special scrutiny, since some of them are already described having antifungal activity.[2] Thiourea was found to occur naturally in laburnum shrubs, and as a metabolite of *Verticillium albo-atrum* and *Bortrylio cinerea*.[3] A literature survey[4] revealed findings of antifungal activity of some thiourea structural analogues (**A** and **B**, Figure 1). Namely, it was reported, that thiosemicarbazone **A** inhibited growth of different *Aspergillus* strains: *A. nomius*, *A. ochraceus*, and *A. parasiticus* with a minimum inhibition concentration (MIC) of 125 μg/mL and of *A. flavus* and *Fusarium verticillioides* with MICs of 250 and 500 μg/mL, respectively.

A comparison of the results of the thiosemicarbazone **A** and other studied semicarbazone antifungals revealed that sulfur instead of

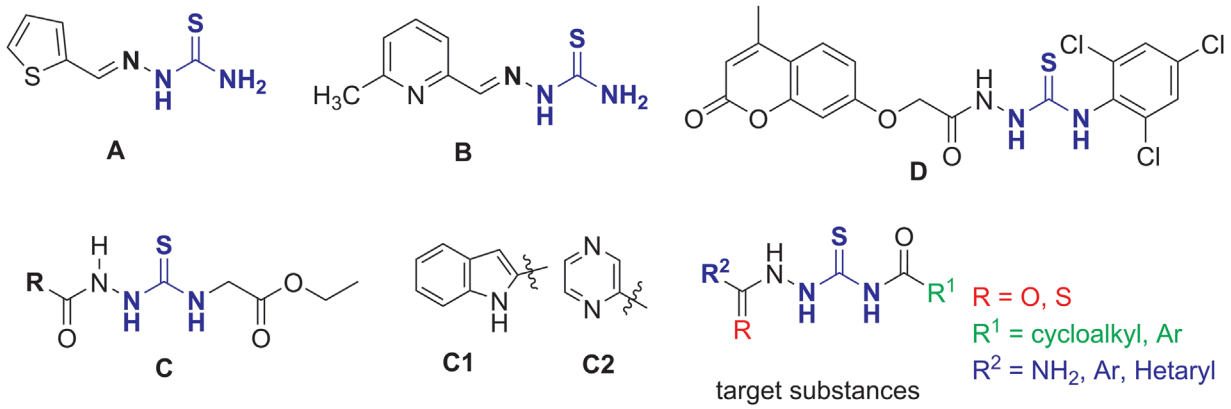

FIGURE 1 Structural analogues (**A–D**) with antifungal activity and substances to be synthesized

oxygen in the core structure conferred a higher activity. Pyrimidine substituted **B** showed antifungal activity against *A. flavus*, *A. parasiticus*, and *F. verticillioides*, but only at an elevated concentration of 500 µg/mL. Among the tested series of compound **C** a complete lack of bioactivity was noted for a derivatives with naphthalene or isoquinoline ring, whereas replacement by smaller indole (**C1**) resulted in a significant antifungal activity (MICs of 200 µg/mL against *C. albicans* and 100 µg/mL against *C. parapsilosis*).[5] An antifungal response was also noted at a higher concentration (MICs > 400 µg/mL toward all screened *Candida* species for pyrazine derivative **C2**, whereas the remaining compounds with five-membered heterocyclic ring were inactive. Siwek et al.[5] also observed that the replacement of an aryl ring in 4-arylthiosemicarbazides with a flexible chain dramatically reduced antifungal response, and that the NH-NH-C(=S)-NH core structure seemed to be important for antifungal activity of thiosemicarbazides. 2-(2-((4-Methyl-2-oxo-2*H*-chromen-7-yl)oxy)acetyl)-*N*-(2,4,6-trichloro-phenyl)hydrazine-1-carbothioamide (**D**) also exhibited moderate antifungal activity (46% of growth inhibition) at 10 µg/mL. Generally, among studied series of coumarinyl thiosemicarbazides, compounds with aromatic substituents showed a better antifungal activity than those with methyl or ethyl rest groups.[6]

Here we describe the synthesis, structure analysis, and antifungal activity of nine novel acyl thioureas (Figure 1, target substances); their potential gene toxicity is analyzed using the *Salmonella* reverse mutagenicity assay (Ames test). Physicochemical drug-likeness descriptors and frontier molecular orbitals energies calculations are applied to estimate potential toxicity. Finally, *in silico* methods are used to evaluate the structure–activity relationship (SAR), and to predict the potential affinity to the most common antifungal enzymatic targets by molecular docking.

2 | RESULTS AND DISCUSSION

2.1 | Chemistry

Preparation of acyl thioureas may be conducted as with isolation of intermediate acyl isothiocyanates,[7] so using insufficient studied one-pot-synthesis method.[8] So, at the first stage of the study, we optimized the synthesis method of compound **8** from accessible reagents (Figure 2).

A one-pot synthesis was easily carried out in acetonitrile with the consecutive addition of equimolecular amounts of ammonium isothiocyanate (80°C for 30 min) and isonicotinic acid hydrazide (80°C for 90 min) to benzoyl chloride with constant stirring. Subsequently, compounds **1**–**7** and **9** were synthesized with satisfactory yields from the acyl chloride of the cyclopropanecarboxylic acid (**a**), ammonium isothiocyanate (**b**) and the corresponding acyl hydrazides ((thio)carbazides) using the given method (Figure 2). This method is selective and characterized by good yields and high purity of the final products.

The purities of compounds were confirmed by LC-MS spectra, structure elucidated by elemental analysis, IR, ^{1}H and ^{13}C NMR spectra.

When characterizing the LC-MS spectra, increasing molecular mass at acyl hydrazidic (**1**–**7**) or thiosemicarbazidic (**9**) fragments and registration of quasimolecular positive ions [M+1] definitely proved the structure of novel compounds.

In ^{1}H NMR-spectra of substances **1**–**9** the characteristic signals of protons were amide (-C(O)N*H*-), thioamide (-(C(S)N*H*-) and acyl hydrazide (-NHN*H*C(O)-R_1) fragments, which were registered at the low field at the 12.69–12.27 ppm, 11.80–11.34 ppm, and 11.34–8.88 ppm, appropriately. The electronic effects of the substituents significantly effected the chemical shift of acyl hydrazide (-NHN*H*C-(O)-R_1) proton's signal.

The protons peaks of cyclopropylic fragment (**1**–**7**) in position 1 were found in the high field as multiplets at the 2.24–1.79 ppm. And signals protons in the second and third positions appeared as broadened multiplets at the 1.18–0.51 ppm. An exception was spectrum of the substance **9**, which had H-1 signal as doublet of triplets with corresponding coupling constants (12.5 and 6.3 Hz). Besides, the spectra of compounds **1** and **9** were characterized by signals of the NH_2 group of carbazide residues at the 6.21 and 7.68 ppm, and compounds **5** and **6** – by signals of the -CH_2 group at the 4.65 and 3.76 ppm, correspondingly. In the ^{1}H NMR spectra of compounds **3**–**8**, also signals of protons from aromatic substituents were recorded, which, depending on the proton environment, had a corresponding multiplicity.

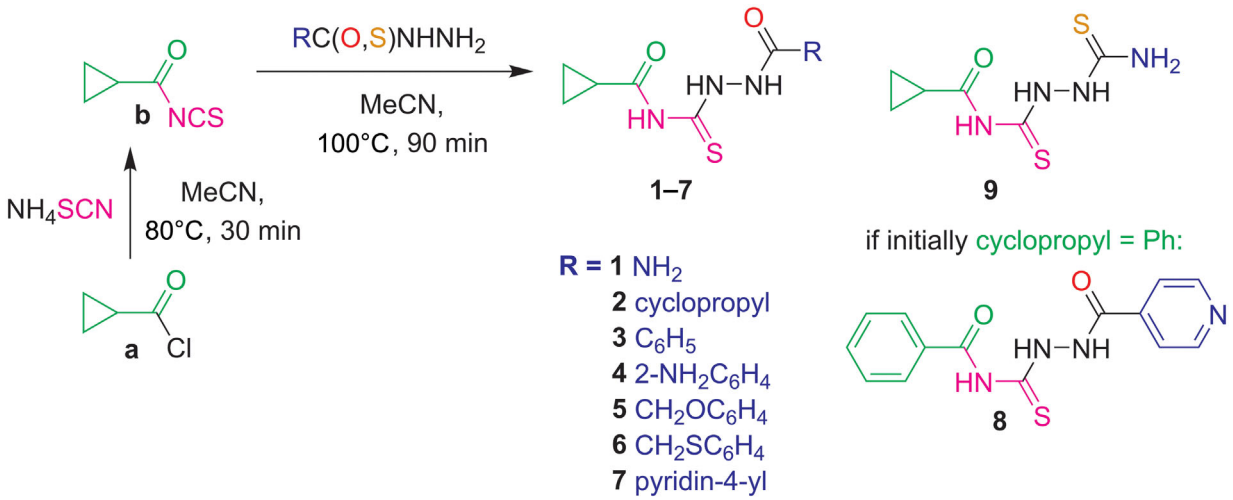

FIGURE 2 Synthetic route of novel *N*-substituted *N*-(hydrazinecarbonothioyl)-cyclopropane-carboxamides **1**–**7**, *N*-(2-isonicotinoylhydrazine-1-carbonothioyl)benzamide (**8**) and *N*-(2-carbamothioylhydrazine-1-carbonothioyl)cyclopropanecarboxamide (**9**)

Uniquely and additionally, the structures of compounds **1**, **5**, and **9** were proven by ^{13}C NMR spectra. Hence, the signals of sp^2-carbon atom were strongly shifted to low field and were registered at the 183.44–178.29 ppm, namely, -C(O)NH<u>C</u>(S)- at the 175.74–175.23 ppm; (-<u>C</u>(O)NHC(S)-) and (-NHNH<u>C</u>(O)-R_1) at the 169.59–156.41 ppm. Besides, the mentioned compounds were characterized by specific signals of sp^3-carbon of cyclopropyl fragment at 14.37–14.27 ppm (C-1) and at 9.87–9.57 ppm (C-2, 3).

2.2 | Antifungal activity

The mycelial growth rate assay[9] was used to determine antifungal activity in different concentrations from 50 to 1 μg/mL. The standard antifungal hymexazol was used as reference. Antifungal activities of nine acyl thioureas and hymexazol against all tested fungi are listed in Table 1.

Notably, *Penicillium digitatum*, *Mucor indicus*, and *Fusarium equiseti* were quite resistant toward acyl thioureas. Nevertheless, with the exception of *F. equiseti*, also hymexazol was inefficient against these strains. Comparing the activity of all acyl thioureas substances **3**, **5**, and **6** were the most effective, even exceeding the activity of hymexazol. They inhibited 9 of 14 studied strains to more than 90% at 50 μg/mL. Also more resistant fungi *Aspergillus niger* (**3**: 67.3%), *Botrytis cinerea* (**3**: 76.4%), and *P. digitatum* (**3**: 55.9%) were susceptible. Remarkably, substance **3** was active against all tested strains with the lowest efficiency against *M. indicus* (28.3%).

The interesting observation also is that in some cases substances with the lowest shown activity (**1**, **4**, **7**) even enhanced the fungi growth (negative values, Table 1). This result should be taken into account for further investigations as growth stimulators.

At a lower concentration range from 25 to 1 μg/mL also significant antifungal activities against at least nine fungi were detected. Again, compounds **3**, **5**, and **6** were among the most effective substances.

Besides, compound **9** was highly active against *Colletotrichum higginsianum*, *Gibberella zeae*, and *Lecanicillium lecanii*; in contrast to substances **3**, **5**, and **6** its activity against other strains was poor. It may be speculated that substance **9** due to different functional groups (Figure 1) targets other physiologically important functions than **3**, **5**, and **6**. So, the average antifungal dosage of majority of substances was lower (10–50 μg/mL) than of reported compounds **A**–**D** (200–500 μg/mL, Figure 1).[4–6]

Since compounds **3**, **5**, and **6** were the most promising, a mixture of 50 μg/mL or 16.6 μg/mL of them was tested against more resistant strains (Figure 3).

With *A. niger* and *F. equiseti* a significant increase of the inhibitory effects was observed when compared with the most active single compound. Interestingly, against *F. equiseti* the mixture was more effective at its lower concentration. With respect to the other tested strains the most active single substance (mostly **3**) was in the same range or even more active as within a corresponding cocktail. A deeper understanding of the molecular mode of action may offer further guidelines how to apply acyl thioureas as mixtures in the most efficient way.

2.3 | SAR

Summing up the obtained data, SAR can be derived with the following traits (Figure 4).

A phenyl ring (**3**), methylenoxyphenyl (**5**) or methylenethio- (**6**) substituent increases the rate and diversity of antifungal activity. Comparing substances **7** and **8**, the replacement of a cyclopropyl ring by a phenyl ring confers an increase of antifungal activity.

Derivatives of acyl thioureas that had pyridine (**7**), 2-amino group in phenyl (**4**) or just an amino group (**1**) exhibited greatly reduced activity. Interestingly, the exchange of a carbonyl oxygen to a sulfur (**1** vs. **9**) has a considerable effect on activity. At the same time, the replacement of oxygen in ether group to sulfur to obtain thioether

TABLE 1 Growth inhibition rate (%) of fungi and *Phytophthora* oomycetes by acyl thiourea derivatives at different concentrations

	CH[a]					FG					VL			FF				FO			
#/µg/mL	50	25	10	5	1	50	25	10	5	1	50	25	10	50	25	10	5	50	25	10	5
3	**100**[b]	**92.6**	**93.3**	**78.6**	17.9	**100**	**92.4**	**90**	**86.2**	56.1	**100**	**100**	39.2	**100**	**94.6**	**83.5**	21.2	**97.6**	**88.3**	**82.1**	−18.9
5	**100**	**93.6**	**79.8**	64.7	22.9	**93.6**	**91**	41.9			**100**	74.4		**100**	**77.4**	42.1		**93.9**	**83.8**	42.1	
6	**100**	**85.7**	**90.1**	57.7	17.9	**94.3**	**91**	32.3			**100**	61.0		**100**	**78.9**	44.2		**100**	49.8		
hym[c]	32.9	8.0	1.6		7.0	34.4	2.1	2.1	−4.0	−2.4	**100**	72.2	68.0	**85.7**	15.4	6.3	4.2	41.6	7.9	2.8	−10.6
8	**75.6**[d]	18.9				63.3					11.9			55.8				58.0			
2	**100**	39.4				**91.9**	59.2				64.3			51.0				31.6			
9	**100**	**100**	**100**	5.0		**100**	18.8				**97.6**	**100**	43.3	30.3				5.7			
7	−5.2					1.3					−2.4			1.6				4.1			
4	3.1					0					−7.1			2.4				0.8			
1	−17.6					0.7					−11.9			1.6				0.8			

	PI GL-1			PI p-3			PI p-4			AA			BC		AN	PD	MI	FE
#/µg/mL	50	25	10	50	25	10	50	25	10	50	25	10	50	25	50			
3	**89.3**	**90.0**	52.6	**89.9**	67.4	55.0	**94.8**	61.8		**91.4**	**75.8**	56.1	**76.4**	0	67.3	55.9	28.3	28.3
5	**85.9**	**81.0**	38.6	**89**	67.4	38.5	**79.0**	15.4		**79.6**	**76.8**	36.5	30.2		68.2	35.7	0	0
6	**92.1**	74.1		**78.8**	50.9	46.7	**84.5**	75.6	72.3	**100**	56.1	31.6	−8.0		66.4	0	0	22.2
hym[c]	51.5			33.2	30.7	6.2	30.4	7.7	2.8	**95.8**	84.5	80.7	**95.6**		17.5	0	0	62.0
8	65.3			64.6			48.8			55.4			−8.0		29.8	0	61.3	0
2	63.2			54.1			53.6			28.1	4.1		−1.5		19.7	14.8	2	0
9	20.6			25.6			40.5			23.5			−7.3		3.6	0	0	0
7	−2.1			7.4			16.5			18.7			−8		−11.1	0	0	0
4	−2.1			7.8			13.1			−11.8			−8.0		−1.8	0	0	0
1	0.7			0.7			10.3			−15.4	0		−8.0		−2.7	0	0	0

[a]Tested strains were *C. higginsianum* (CH), *F. graminearum* (FG), *V. lecanii* (VL), *F. fujikuroi* (FF), *F. oxysporum* (FO), *P. infestans* GL-1 01/14 wild strain (PI-GL 1), *P. infestans* p-3 (PI p-3), *P. infestans* p-4 (PI p-4), *A. alternata* (AA), *B. cinerea* (BC), *A. niger* (AN), *P. digitatum* (PD), *M. indicus* (MI), *F. equiseti* (FE).

[b]100: no growth observed. Substances numbering order in columns is given by the average activity decrease.

[c]hym: hymexazol.

[d]Bold figures designate inhibition rates >75%; negative values designate growth stimulations (i.e., enlarged growth zone compared to control).

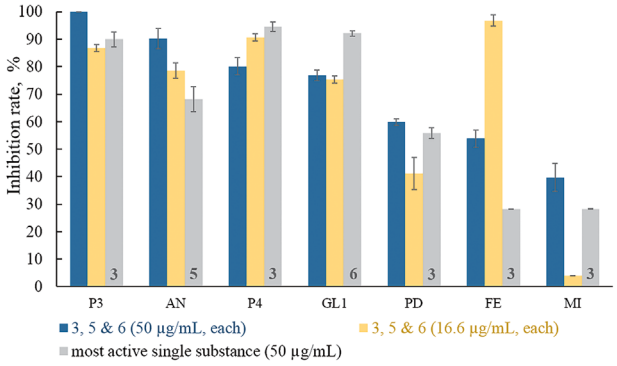

FIGURE 3 Antifungal activity of acyl thiourea mixtures. Acyl thiourea derivatives **3**, **5**, and **6** were applied as a mix of 50 µg/mL (each) or 16.6 µg/mL (each) and compared to the single compound (inlet number) which gave the highest activity (Table 1). Designation of strains is as in Table 1. Data represent means and standard deviations (error bars) from experiments carried out in triplicate. All other experimental procedures were as described in Experimental part

(**5** vs. **6**) does not alter the activity. In these structures, the electron density and delocalization of the phenyl ring probably prevented interaction with enzymatic targets of the mentioned atoms.

Future chemical modification to enhance the antifungal potential should include phenyl ring systems impact, e.g., methylenoxyphenyl or methylenethiophenyl rest groups, or aryls with electron withdrawing substituents from hydrazide site of acyl thioureas with thiosemicarbazide fragment instead of semicarbazide one (Figure 4).

2.4 | *Salmonella* reverse mutagenicity test

The detected antifungal activity renders acyl thioureas to an attractive starting point to develop them as useful agrochemicals, which may come into widespread contact to farm operators and the environment. An evaluation of their safety must therefore be an integral part of this development. Here the potential gene-toxicity, which often associates with mutagenicity, was analyzed applying the *Salmonella* reverse mutagenicity assay ("Ames test").[10] Frame shift (TA 98) and base substitution (TA 100) *his*$^-$ mutated *Salmonella* test strains were challenged with acyl thioureas at doses of 50 or 500 µg/plate. Substances were also analyzed in the presence of rat liver extract ("S9-mix") in order to simulate potential metabolic activation. Grown colonies of revertants (reverse mutations) were counted after 48 h incubation on a minimal agar medium. As an indication of gene toxicity a mutagenic index (M_i; ratio of colony number of revertants in the presence of test compound vs. revertants of negative control (i.e., spontaneous reversion rate)) exceeding 2 was set.[10,11]

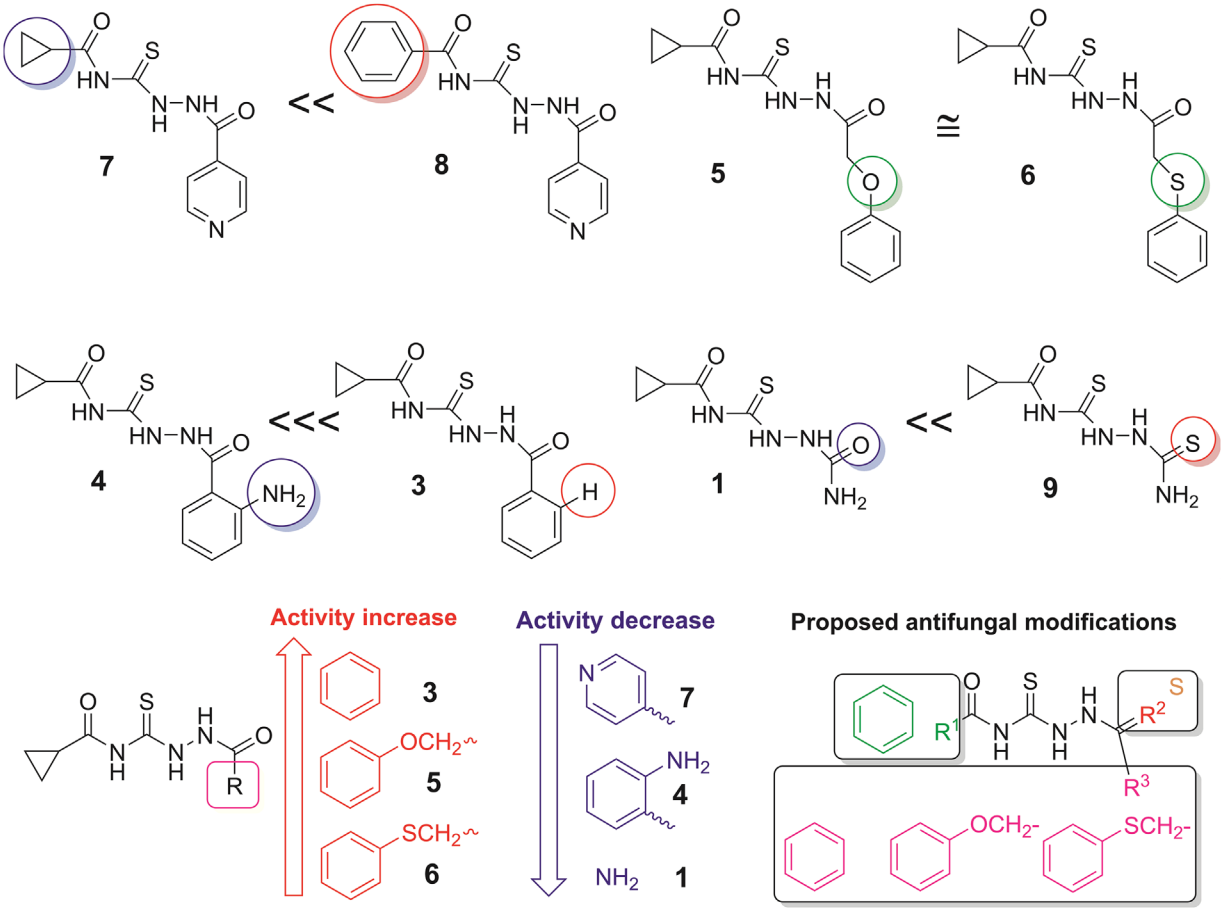

FIGURE 4 Structure–antifungal activity relationship of novel acyl thioureas

In all tests the mutagenicity index was below 2, i.e., the number of revertants did not increase; also in the presence of S9-mix a mutagenic effect was not observed (Table 2).

A 10-fold increase in the substance amount to 500 µg per plate revealed a biocidal effect against *Salmonella* for all substances except for **1**, **7**, and **9**. With these compounds there was no dose-dependent correlation in the number of revertants. At a dose of 500 µg/plate the inclusion of S9-mix lowered the amount of revertants for TA 100. The significance of this finding is difficult to evaluate since at this high dose bactericidal effects may interfere with mutagenic effects. Generally, it may be assumed that oxidation of amino group mediated by cytochrome P450 of S9-mix could lead to formation of highly mutagenic *N*-hydroxylamines, nitroso compounds or nitrenium ions.[12,13] Nevertheless, we did not find any evidence that S9-mix was active in this sense. Therefore, according to our test results we classify novel thiourea derivatives as "non-mutagenic" so far.

2.5 | Physicochemical characteristics

2.5.1 | Drug likeness

Substance promiscuity and frontier orbitals energies are physico-chemical parameters to get an in-depth understanding of biological activity and drug likeness of novel substances.[14,15] If two or more of "drug-like" requirements are not met, there is a high probability of poor bioavailability for the drug candidate[16–20] (Table 3). So, if the molecular weight (MW) is less than 500 g/mol, it may penetrate through biological membranes more easily and rapidly, may have a minimum number of undesirable targeting adhesions, and therefore has less toxic side effects. Hydrogen bond donor (HBD) and acceptor (HBA) numbers indicate the compound's tendency to form hydrogen bonds and to dissolve in water. When the value is high, the adhesion to biological targets could become too strong and cause pathological changes for organism. If the logarithm of the substance distribution ratio (log D) between *n*-octanol and water is below −0.5, the substance does not dissolve in the lipid phase and penetrate through the cell membrane, i.e., it will lose the ability to be absorbed into the blood stream from the gastrointestinal tract. As far as studied acyl thioureas are ionizable substances, the log D was calculated assuming different levels of pH (3.0, 7.4, and 9.0).[21] Special attention was given to pH = 7.4 considering it is the H^+ concentration of human plasma. The topological polar surface area (TPSA) of a molecule is defined as the surface sum over all polar atoms, showing a low permeability through cell membranes, when it is larger than 140 angstroms^2 (Å^2).[22] In order to penetrate through the blood–brain barrier, a TPSA must be less than 90 Å^2.[23] But when lower than 75 Å^2 it associates with an increased

TABLE 2 Mutagenicity indexes (M_i) calculated from numbers of revertants

		TA 98		TA 100	
Substances	**Dosage, µg/plate**		**+S9-mix**		**+S9-mix**
2-Nitrofluorene	10	58.40			
Methyl methansulfonate	1			8.34	
2-Aminofluorene	10	1.56	47.35	1.01	4.58
1	50	0.60	0.55	1.82	0.76
	500	0.73	0.88	1.17	0.69
2	50	0.84	1.12	1.36	0.90
	500	ng	ng	ng	ng
3	50	0.66	0.52	1.39	0.67
	500	ng	ng	ng	ng
4	50	0.66	0.75	1.37	0.94
	500	ng	0.13	ng	ng
5	50	0.60	0.95	1.81	0.82
	500	0.02	0.05	ng	ng
6	50	0.57	0.66	1.58	0.84
	500	ng	ng	ng	ng
7	50	0.73	1.12	1.64	0.96
	500	0.55	0.52	0.63	0.42
8	50	0.76	1.07	1.58	0.78
	500	0.06	ng	ng	ng
9	50	0.60	0.81	0.95	0.74
	500	0.60	0.68	1.84	1.00

Substances for positive controls and acyl thioureas (**1**–**9**) were solved in DMSO; all assays, including negative controls (spontaneous reversion rate), were carried out with 100 µL DMSO in top agar. For M_i calculations mean numbers were taken from experiments carried out in triplicate. ng, no growth.

TABLE 3 Calculated parameters of lead-like and structure optimization

#	SMILES	MW	Log D pH = 3	Log D pH = 7.4	Log D pH = 10	TPSA	HBA	HBD	nrotb
1	NC(=O)NNC(=S)NC(=O)C1CC1	202.24	−0.63	−0.63	−1.18	96.25	6	5	4
2	O=C(NNC(=S)NC(=O)C1CC1)C2CC2	227.29	0.48	0.48	−0.05	70.22	5	3	5
3	O=C(NC(=S)NNC(=O)C1=CC=CC=C1)C2CC2	263.32	1.56	1.56	0.91	70.22	5	3	5
4	NC1=CC=CC=C1C(=O)NNC(=S)NC(=O)C2CC2	278.34	1.23	1.38	0.79	96.25	6	5	5
5	O=C(COC1=CC=CC=C1)NNC(=S)NC(=O) C2CC2	293.35	1.22	1.22	0.67	79.46	6	3	7
6	O=C(CSC1=CC=CC=C1)NNC(=S)NC(=O) C2CC2	309.42	1.70	1.70	1.16	70.22	5	3	7
7	O=C(NC(=S)NNC(=O)C1=CC=NC=C1)C2CC2	264.31	0	0.34	−0.43	83.11	6	3	5
8	O=C(NNC(=S)NC(=O)C1=CC=CC=C1) C2=CC=NC=C2	300.34	1.07	1.41	0.78	83.11	6	3	5
9	NC(=S)NNC(=S)NC(=O)C1CC1	218.31	0.26	0.26	−0.27	79.17	5	5	5
Drug lead-like criteria		≤500	≤5			≤140	≤10	≤5	≤10

SMILES, simplified molecular input line entry system; MW, molecular weight; Log D, *n*-octanol/water distribution coefficient; TPSA, molecular polar surface area; HBA, hydrogen bonds acceptors; HBD, hydrogen bonds donors; nrotb, number of rotatable bonds.

risk of adverse effects due to non-specific toxicity, particularly when combined with a high lipophilicity (log D > 4). An increase in the number of rotatable bonds (nrotb) increases free rotation axes of the molecule and thereby provides an enhanced flexibility.

As calculations revealed (Table 3), all substances do not violate drug-like criteria and fulfill the requirements of the bioavailability rules.[18–20]

Still there are some aspects worth to be discussed: the molecular TPSAs for all acyl thioureas were not more than 140 Å^2, but lower than 75 Å^2 for substances **2**, **3**, and **6**; these could possibly penetrate the blood brain barrier. Compounds **1**, **4**, and **9** have the limit amount of HBD (5) and could remain in the cell due to strong hydrogen bonding. At pH = 7.4 substance **1** is quite hydrophilic with a log D of −0.63. At the same pH compounds **2**, **7**, and **9** have the lowest lipophilicity (log D = 0.48, 0.34, and 0.26, respectively). In contrast, **3**, **5**, and **6** appeared as the most penetrable ones, due to highest lipophilicity and lowest TPSA. It is notable that these above-mentioned profiles correlate with their distinctive antifungal activity.

2.5.2 | Promiscuity

The next analysis was to determine how far acyl thioureas may categorize as "Pan Assay Interference Compounds" (PAINS).[24] PAINS are compounds that turn up as frequent hitters in many biochemical high-throughput drug discovery screens and so look as promising starting point for further drug development. Unfortunately, often these substances are "promiscuous," i.e., reacting simultaneously with many targets in a non-specific or even indirect mode.[25] Correspondingly, substances were screened by means of bioactivity data using an associative promiscuity pattern learning engine[26,27] (Table 4). The pScore column points to promiscuity, whereas "inDrug" column indicates whether the corresponding molecular scaffold exists within any approved drug (true means it was found in the base; and false − not found). A high pScore value combined with a "true" inDrug finding are strong predictors to an enhanced promiscuity and potential toxicity.

Such an analysis revealed that pyridine scaffolds of **7** and **8** have a pScore higher than 300 (Table 4). Taking under consideration the presence of pyridine in their structure, a mutagenic potential can be assumed. At least this was not confirmed by bacterial mutagenicity analysis (Table 2). Since compounds **7** and **9** showed low antifungal activity, they will not be taken under consideration for further antifungal studies. The substances **5** and **8** had pScore/inDrug profile determined as low/false. The pScores of **1**–**7** and **9** are calculated as moderate (185) reflecting the presence of the cyclopropyl ring. Calculating the promiscuity of **2**–**4**, **6**, and **7** no data were generated, which meant a neutral result with respect to toxicity prediction. Still lacking heterocyclic rings the substances are assumed to have a low toxicity profile.

2.5.3 | Frontier molecular orbitals energy

Next, molecular mechanics, namely, calculations of the frontier molecular orbitals energies to predict substances toxicity by HOMO

TABLE 4 Calculated promiscuity scores by bioactivity data associative promiscuity pattern learning engine

Substance	Scaffold	pScore	inDrug
1–7, **9**	Cyclopropane	185 (moderate)	True
5	Whole molecule	30 (low)	False
8	Whole molecule	2 (low)	False
7, **8**	Pyridine	328 (high)	True

False, not found in reported drug; true, found.

(highest occupied molecular orbital) and LUMO (lowest unoccupied molecular orbital) (Table 5) were carried out.[14,28] Also energy gap and molecular descriptors computed at the level of semiempirical molecular mechanics (MM+ and MNDO (modified neglect of diatomic overlap)) by the means of HyperChem Professional 8.0[29] are shown as bioactivity indicators.

The binding ability of the molecule gets stronger with increasing HOMO and decreasing LUMO energy values. If LUMO energy is negative, the substance is considered electrophilic. When the HOMO–LUMO energy gap (ΔE) increases, the molecule becomes harder (η), more stable and less reactive. Vice versa, the higher the electronegativity (χ) and the electronic chemical potential (μ), the less stable or more reactive the molecule will be. Electrophilicity index (ω) is also an indicator of the stabilization in energy after a system accepts additional amount of electronic charge from the environment. A highly bioactive substance typically has an elevated electrophilicity index and low hardness. As it is shown in Table 5, the studied substances are not highly reactive hard electrophiles. According to the index of electrophilicity, substances **7–9** are predicted as the most bioreactive among tested series. In contrast they are low with antifungal activity, and therefore are not in the focus of future antifungal studies.

2.6 | Molecular docking studies

Analysis of the *in silico* molecular docking analysis[30] was used as a tool to predict affinity scores of hymexazol and acyl thioureas **1**–**9** to common antifungal targets[5] (Table 6).

The 14α-demethylase (CYP51) and *N*-myristoyltransferase (NMT) are found to be possible target enzymes for lead-compounds **3** and **5** according to their best affinity scores (−7.8 to −8.2) (Table 6). This finding is in agreement with earlier studies of antifungal activity of thiosemicarbazides.[5]

The visualization obtained by molecular docking results indicates (Figure 5) that substance **3** binds to CYP51 due to the presence of a hydrogen bond between sulfur and MET A:508 (3.72 Å), π-alkyl bonds of cyclopropyl fragment with TYR A:132 and A:118 (4.97 and 3.58 Å) and two unfavorable positive–positive repulsion of the phenyl ring and HEM-nitrogen A:601 (3.98 and 4.78 Å). Additionally, substance **3** also interacts with GLY A:307 and LEU A:376 of target due to van der Waals attraction.

The binding of substance **5** is similar to substance **3** with some additional aspects: a further hydrogen bond is predicted between protonated nitrogen and GLY A:307 (2.70 Å). Besides a third hydrophobic π-alkyl bond is found between cyclopropyl and LEU A:121 (5.48 Å). Also the same type of bond is demonstrated for phenyl ring with ILE A:131 (5.01 Å) in parallel to π-sigma one with HEM A:601 (3.80 Å). Also van der Waals interactions with VAL A:509, PHE A:228, and LEU A:376 are shown.

Considering *N*-myristoyltransferase enzyme, two times more bonds are predicted (Figure 6) with substances **3** or **5**.

Compound **3**, it forms a hydrogen bond with sulfur by TYR B:354 (3.78 Å), π-sulfur bond with PHE B:117 (5.06 Å). LEU B:451 binds to three positively charged nitrogens (2.20, 4.07, and 4.19 Å) due to electrostatic attractive charge interaction. Also cyclopropyl interacts with two TYR B:119 (5.47 Å) and B:107 (4.43 Å), LEU B:337 (3.85 Å) by alkyl bonding. π–π T-shaped bond is shown between TYR B:225 (4.97 Å) and phenyl ring, with additionally π-σ type to LEU B:394 (3.64 Å). Additionally, compound **3** binds by three van der Waals interactions comprising LEU B:415; B:450, and TYR B:335.

Substance **5** fits into the enzyme active site due to two conventional hydrogen bonds between sulfur and THR B:211 (4.46 Å), oxygen and TYR B:335 (2.93 Å). Further interactions are predicted: carbon hydrogen bond of O<u>C</u>H$_2$ fragment with LEU B:450 (3.75 Å), attractive charge type of nitrogen with LEU B:451 (3.15 Å), three alkyl bonds to cyclopropyl by TYR B:107 (4.68 Å), PHE B:117 (3.84 Å) and LEU B:337 (5.18 Å), π-σ bond by LEU B:394 (3.64 Å), two π–π T-shaped bonds by TYR B:354 (5.36 Å) and B:225 (5.13 Å) to the phenyl ring. But, surprisingly, no van der Waals attractions were present.

TABLE 5 Frontier molecular orbitals

#	HOMO −1 MO	HOMO/ |ionization potential|	LUMO/ |electron affinity|	LUMO +1 MO	Energy gap, ΔE	Electrochem. potential, μ, |electronegat., χ|	Hardness, η	Softness, σ	Electrophilicity index, ω
1	−9.6533	−9.4418	−0.7390	0.5070	8.7028	5.09	4.35	0.23	2.98
2	−9.5638	−9.2448	−0.5587	0.2751	8.6861	4.90	4.34	0.23	2.77
3	−9.6172	−9.3720	−0.6992	−0.4345	8.6727	5.04	4.34	0.23	2.92
4	−9.2885	−9.2428	−0.6146	−0.4159	8.6282	4.93	4.31	0.23	2.82
5	−9.5897	−9.1785	−0.8196	0.0918	8.3589	5.00	4.18	0.24	2.99
6	−9.5851	−9.5536	−0.7934	−0.2975	8.7602	5.17	4.38	0.23	3.06
7	−10.0023	−9.5875	−0.8866	−0.5951	8.7009	5.24	4.35	0.23	3.15
8	−9.5560	−9.8320	−0.7814	−0.4916	9.0506	5.31	4.53	0.22	3.11
9	−9.2455	−9.0340	−0.9731	−0.1738	8.0609	5.00	4.03	0.25	3.11
Hymexazol	−10.4157	−10.1161	−0.1170	−0.9532	9.9992	5.12	5.00	0.20	2.62

Energies of frontier molecular orbitals, the energy gap and molecular descriptors computed at the level of semi-empirical MM+ and MNDO Hamiltonians, eV.

TABLE 6 Affinity to binding sites

	Affinity, kcal/mol						
	Candida albicans			*Escherichia coli*		*Sacchromyces cerevisiae*	
Sub.	5TZ1	1IYL	1EAG	1UAG	1XFF	1Q1D	Mean
Hymexazol	−4.3	−5.0	−3.9	−4.4	−5.1	−4.6	−4.6
1	−6.1	−6.1	−5.7	−6.4	−6.3	−6.3	−6.2
2	−6.9	−6.6	−6.0	−5.9	−6.0	−6.5	−6.3
3	−8.2	−7.8	−7.1	−6.5	−5.6	−6.4	−6.9
4	−8.2	−7.6	−7.0	−6.8	−5.6	−6.4	−6.9
5	−8.1	−7.8	−7.3	−6.6	−6.3	−6.2	−7.1
6	−8.0	−7.7	−7.1	−6.8	−6.2	−5.8	−6.9
7	−7.7	−7.1	−6.3	−6.6	−5.5	−5.8	−6.5
8	−8.8	−9.1	−7.4	−7.3	−6.0	−7.1	−7.6
9	−5.6	−5.7	−5.3	−5.7	−5.9	−6.2	−5.7
Mean for **1–9**	−7.5	−7.3	−6.6	−6.5	−5.9	−6.3	–

The calculated affinity of substances to binding sites of sterol 14α-demethylase (CYP51) 5TZ1, *N*-myristoyltransferase (NMT) 1IYL, secreted aspartic proteinase (SAP2) 1EAG, UDP-*N*-acetylmuramoyl-L-alanine:D-glutamate ligase (MurD) 1UAG, L-glutamine:D-fructose-6-phosphate amidotransferase (GlcN-6-P) 1XFF and topoisomerase II (Topo II) 1Q1D.

A 3-D fit of substances within above-mentioned enzymes active sites is shown on the right of Figures 5 and 6.

2.7 | Correlation activity – structural descriptors

Correlation coefficients were determined between average antifungal properties of each acyl thiourea derivative and its calculated descriptors in order to identify those parameters having the highest impact on the activity presence for tested series of compounds (Table 7).

The highest correlation coefficient was found between average antifungal activity of each substance and their TPSA (0.6672), whereas MW influenced much less (R^2 = 0.2093). Also protonation at pH = 3 caused the moderate result of correlation − 0.5339, and deprotonation

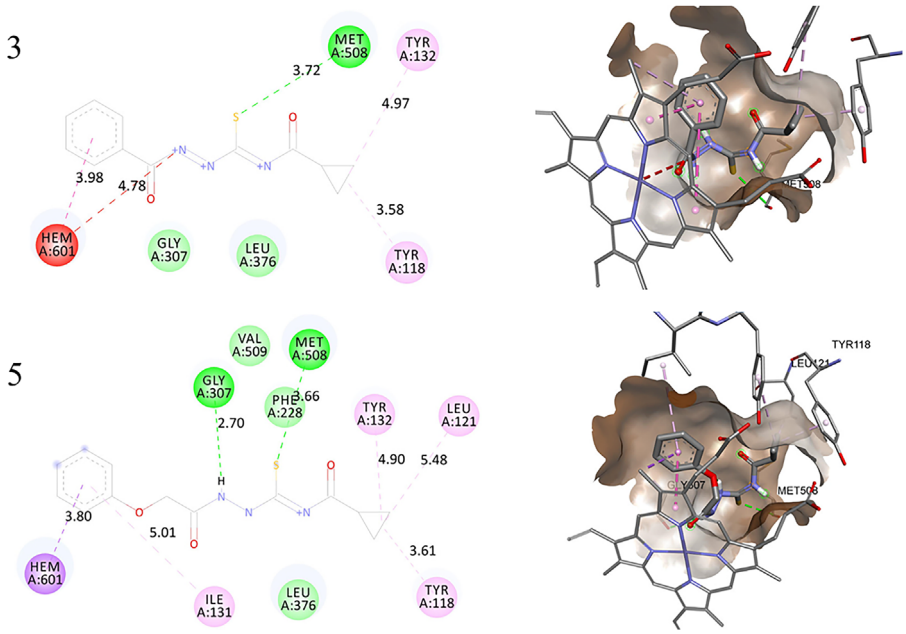

FIGURE 5 Visual representation (2D and 3D) of the lead compounds **3** and **5** showing bonds formation and position in the active site of 14α-demethylase (5TZ1). Red − unfavorable positive–positive interaction, pale green − van der Waals interaction, green − classical conventional hydrogen bond, violet − hydrophobic π-σ bond, pink − hydrophobic alkyl and π-alkyl bonds

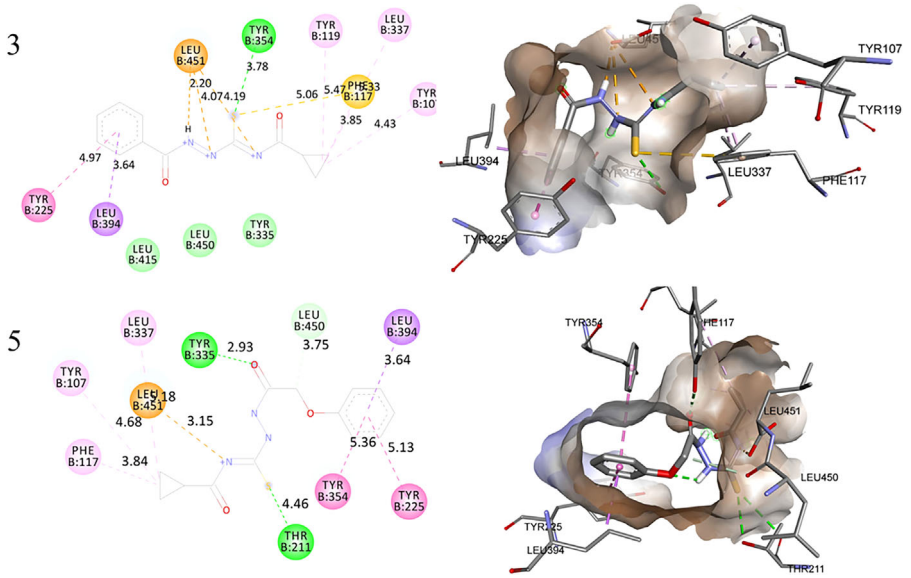

FIGURE 6 Visual representation (2D and 3D) of the lead-compounds **3** and **5** showing bonds formation and position in the active site of *N*-myristoyltransferase (1IYL). Pale green – van der Waals interaction, green – classical conventional hydrogen bond, light blue – non-classical carbon hydrogen bond, dark orange – electrostatic attractive charge interaction, light orange – miscellaneous π-sulfur bond, violet – hydrophobic π-σ bond, magenta – hydrophobic π–π T-shaped bond, pink – hydrophobic alkyl and π-alkyl bonds

at pH = 10 lead to decrease of R^2 with 0.4575. And at pH = 7.4, R^2 was the lowest among them (0.4250). Electrophilicity was not linearly related to detected antifungal activity. Among enzymatic targets affinity to SAP2 had the highest correlation to found antifungal properties (0.2551).

Lipophilic compounds with low-energy LUMOs are considered likely to be mutagenic, hence possibly carcinogenic.[31–33] Therefore, this parameter was also calculated against found results (mean of M_i-values of all acyl thioureas of both tester strains with/without S9-mix, respectively; Table 2) from *Salmonella* mutagenicity assay. Only to the frame-shift mutated TA98 strain a weak correlation (0.2191) with the LUMO was detected. This result confirms our finding of the absence of a mutagenic potential of this series of acyl thioureas.

3 | CONCLUSION

Among nine novel acyl thioureas potent non-mutagenic antifungal substances with a low toxicity profile were identified, which warrant follow-up studies: further investigations of antifungal activity of active

TABLE 7 Correlation coefficients between average antifungal activity of **1–9** to their calculated physico-chemical descriptors, and LUMO to mutagenicity or lipophilicity results

Average antifungal activity against							
			Log D at pH				
Descriptor	**MW**	**TPSA**	**3**	**7.4**	**10**		**Electrophilicity index**
R^2	0.2093	0.6672	0.5339	0.4250	0.4575		0.0181
Affinity							
Enzyme	**CYP51**	**NMT**	**SAP2**	**Topo II**	**MurD**		**GlcN-6-P**
R^2	0.1368	0.1684	0.2551	0.0030	0.0034		0.0597
LUMO energy against							
	TA 98, 50 µg/plate		**TA 100, 50 µg/plate**		**Log D at pH**		
***Salmonella* strain/descriptor**		**+ S9**		**+ S9**	**3**	**7.4**	**10**
R^2	0.2191	0.0048	0.0114	0.0524	0.0441	0.0315	0.0390

MW, molecular weight; TPSA, molecular topological polar surface area; Log D, distribution coefficient; *Salmonella* strain TA 98 and TA 100 without and with addition of S9-mix; affinity to 14α-demethylase (CYP51), *N*-myristoyltransferase (NMT), secreted aspartic proteinase (SAP2), topoisomerase II (Topo II), UDP-*N*-acetyl-muramoyl-L-alanine:D-glutamate ligase (MurD), L-glutamine:D-fructose-6-phosphate aminotransferase (GlcN-6-P), LUMO, energy of lowest unoccupied molecular orbital.

substance mixtures to broaden spectrum of their properties; ecotoxicity tests for lead substances **3**, **5**, and **6** to be used in agriculture; antifungal spectrum widening to human pathogens for active compounds; chemical modification of the main core according to SAR results; studies of *in vitro* enzymatic affinity to validate the predicted interactions with target structures as identified by docking studies.

4 | EXPERIMENTAL

4.1 | Chemistry

4.1.1 | General

Melting points were determined in open capillary tubes and were uncorrected. The elemental analyses (C, H, N, S) were performed using a vario EL Cube analyzer (Elementar Americas, NJ, USA). Analyses were indicated by the symbols of the elements or functions within ±0.3% of the theoretical values. The ^{1}H NMR spectra (400 MHz) were recorded on a Varian-Mercury 400 (Varian Inc., Palo Alto, CA, USA) spectrometer with TMS as an internal standard in DMSO-d_6 solution. LC-MS were recorded using the chromatography/mass spectrometric system consisting of an "Agilent 1100 Series" high performance liquid chromatograph (Agilent, Palo Alto, CA, USA) equipped with an "Agilent LC/MSD SL" diode-matrix.

Starting materials and solvents were obtained from commercially available sources and used without additional purification.

IR, LC-MS and ^{1}H, ^{13}C NMR spectra of the novel substances **1–9** are provided as Supporting Information. The InChI codes of the investigated compounds together with some biological activity data are also provided as Supporting Information.

4.1.2 | General procedure for the synthesis of substances 1–9

To a solution of proper chloroanhydrides (0.01 mol) in 20 mL of acetonitrile 0.76 g of ammonium isothiocyanate (0.01 mol) was added and stirred at 80°C for 30 min. The mixture was cooled down to r.t. and 0.01 mol of proper acylhydrazide, or hydrazinecarboxamide, or hydrazinecarbothioamide was added and stirred at 80°C for further 90 min. The solution was cooled down, poured into the water and the formed precipitate was filtrated, dried, and recrystallized from methanol.

2-((Cyclopropanecarbonyl)carbamothioyl)hydrazine-1-carboxamide (1)

Yield: 75.2%; mp 199–201°C; IR (cm^{-1}): 3212, 1692, 1504, 1395, 1233, 1186, 1153, 1074, 1031, 945, 882, 763, 710, 668; ^{1}H NMR, δ, ppm (*J*, Hz): 12.56 (s, 1H, C(O)NHC(S)-), 11.45 (s, 1H, -C(S)NHNHC(O)-), 8.88 (s, 1H, -C(S)NHNHC(O)-), 6.21 (s, 2H, NH_2), 2.14–1.93 (m, 1H, Cpr H-1), 1.02–0.77 (m, 4H, H-2,2′,3,3′); ^{13}C NMR, δ, ppm: 183.44 (-C(O)NHC(S)-), 175.57 (-C(O)NHC(S)-), 156.41 (NHC(O)NH_2), 14.27 (Cpr C-1), 9.57 (Cpr C 2,3); LC-MS: *m/z* = 203 [M+1], 204 [M+2]. Anal. calcd. for $C_6H_{10}N_4O_2S$: C, 35.64; H, 4.98; N, 27.70; S, 15.85. Found: C, 35.72; H, 5.05; N, 27.76; S, 15.89.

***N*-(2-(Cyclopropanecarbonyl)hydrazine-1-carbonothioyl)-cyclopropanecarboxamide (2)**

Yield: 52.6%; mp 192–192°C; IR (cm^{-1}): 3193, 1683, 1651, 1391, 1138, 1102, 940, 882, 866, 818, 709, 676, 642; ^{1}H NMR, δ, ppm (*J*, Hz): 12.58 (s, 1H, -C(O)NHC(S)-), 11.58 (s, 1H, -C(S)NHNHC(O)-), 10.77 (s, 1H, -C(S)NHNHC(O)-), 2.13–1.98 (m, 1H, cyclopropanecarboxamide H-1), 1.93–1.79 (m, 1H, cyclopropanecarbonylhydrazine, H-1), 1.15–0.51 (m, 8H, cyclopropanecarboxamide H-2,2′,3,3′, cyclopropanecarbonylhydrazine H-2,2′,3,3′); LC-MS: *m/z* = 228 [M+1]. Anal. calcd. for $C_9H_{13}N_3O_2S$: C, 47.56; H, 5.77; N, 18.49; S, 14.11. Found: C, 47.67; H, 5.65; N, 18.54; S, 14.18.

***N*-(2-Benzoylhydrazine-1-carbonothioyl)cyclopropanecarboxamide (3)**

Yield: 75.4%; mp 204–206°C; IR (cm^{-1}): 3230, 1627, 1519, 1455, 1290, 1217, 1155, 950, 912, 707, 670, 619; ^{1}H NMR, δ, ppm (*J*, Hz): 12.40 (s, 1H, −C(O)NHC(S)-), 11.76 (s, 1H, -C(S)NHNHC(O)-), 10.81 (s, 1H, -C(S)NHNHC(O)-), 7.91 (d, *J* = 7.2, 2H, Ph H-2,6), 7.54 (t, *J* = 7.2, 1H, Ph H-4), 7.46 (t, *J* = 7.1, 2H, Ph H-3,5), 2.22–1.93 (m, 1H, Cpr H-1), 1.18–0.75 (m, 4H, Cpr H-2,2′,3,3′); LC-MS: *m/z* = 264 [M+1], 265 [M+2]. Anal. calcd. for $C_{12}H_{13}N_3O_2S$: C, 54.74; H, 4.98; N, 15.96; S, 12.18. Found: C, 54.79; H, 5.04; N, 16.02; S, 12.22.

***N*-(2-(2-Aminobenzoyl)hydrazine-1-carbonothioyl)-cyclopropanecarboxamide (4)**

Yield: 81.6%; mp 187–189°C; IR (cm^{-1}): 3155, 1652, 1515, 1390, 1158, 931, 668; ^{1}H NMR (DMSO-d_6), δ, ppm (*J*, Hz): 12.52 (s, 1H, -C(O)NHC(S)-), 11.74 (s, 1H, -C(S)NHNHC(O)-), 7.95–7.62 (m, 2H, NH_2), 7.53 (d, *J* = 7.7, 1H, Ar H-6), 7.15 (t, *J* = 7.6, 1H, Ar H-4), 6.72 (d, *J* = 8.2, 1H, Ar H-3), 6.53 (t, *J* = 7.4, 1H, Ar H-5), 2.24–1.95 (m, 1H, Cpr H-1), 1.12–0.79 (m, 4H, Cpr H-2,2′,3,3′); LC-MS: *m/z* = 279 [M+1], 280 [M+2]. Anal. calcd. for $C_{12}H_{14}N_4O_2S$: C, 51.78; H, 5.07; N, 20.13; S, 11.52. Found: C, 51.82; H, 5.11; N, 20.18; S, 11.56.

***N*-(2-(2-Phenoxyacetyl)hydrazine-1-carbonothioyl)-cyclopropanecarboxamide (5)**

Yield: 70.8%; mp 194–196°C; IR (cm^{-1}): 1651, 1549, 1472, 1441, 1394, 1224, 1158, 1036, 936, 885, 836, 749, 668, 628; ^{1}H NMR, δ, ppm (*J*, Hz): 12.62 (s, 1H, -C(O)NHC(S)-), 11.77 (s, 1H, -C(S)NHNHC(O)-), 10.73 (s, 1H, -C(S)NHNHC(O)-), 7.27 (t, *J* = 7.8, 2H, Ph H-3,5), 7.01–6.85 (m, 3H, Ph H-2,4,6), 4.65 (s, 2H, -CH_2OPh), 2.16–1.98 (m, 1H, Cpr H-1), 1.04–0.66 (m, 4H, Cpr H-2,2′,3,3′); ^{13}C NMR, δ, ppm: 178.29 (-C(O)NHC(S)-), 175.74 (C(O)NHC(S)-), 165.59 (-C(S)NHNHC(O)-), 158.11 (Ph C-1), 129.96 (Ph C-3,5), 121.77 (Ph C-4), 115.18 (Ph C-2,4), 66.02 (-CH_2OPh), 14.37 (Cpr. C-1), 9.87 (Cpr. C-2,3). LC-MS: *m/z* = 294 [M+1], 295 [M+2]. Anal. calcd. for $C_{13}H_{15}N_3O_3S$: C, 53.23; H, 5.15; N, 14.32; S, 10.93. Found: C, 53.29; H, 5.22; N, 14.38; S, 10.97.

***N*-(2-(2-(Phenylthio)acetyl)hydrazine-1-carbonothioyl)-cyclopropanecarboxamide (6)**

Yield: 76.4%; mp 187–189°C; IR (cm^{-1}): 1680, 1643, 1436, 1386, 1213, 1156, 873, 738, 670; ^{1}H NMR, δ, ppm (*J*, Hz): 12.69 (d, *J* = 5.0, 1H, -C(O)NHC(S)-), 11.68 (s, 1H, -C(S)NHNHC(O)-), 10.99 (d, *J* = 4.9,

1H, -C(S)NHNHC(O)-), 7.40 (d, *J* = 7.6, 2H, Ph-H 2,6), 7.28 (t, *J* = 7.6, 2H, Ph H-3,5), 7.17 (t, *J* = 7.2, 1H, Ph H-4), 3.76 (s, 2H, -CH_2SPh), 2.18–1.96 (m, 1H, Cpr. H-1), 1.20–0.68 (m, 4H, Cpr H-2,2′,3,3′); LC-MS: *m/z* = 310 [M+1], 312 [M+3]. Anal. calcd. for $C_{13}H_{15}N_3O_2S_2$: C, 50.47; H, 4.89; N, 13.58; S, 20.72. Found: C, 50.53; H, 4.93; N, 13.64; S, 20.79.

N-(2-Isonicotinoylhydrazine-1-carbonothioyl)-cyclopropanecarboxamide (7)

Yield: 72.3%; mp 183–186°C; IR (cm^{-1}): 2846, 1655, 1472, 1217, 1162, 1113, 944, 910, 870, 735, 674; ^{1}H NMR, δ, ppm (*J*, Hz): 12.27 (s, 1H, -C(O)NHC(S)-), 11.80 (s, 1H, -C(S)NHNHC(O)-), 11.20 (s, 1H, -C(S)NHNHC(O)-), 8.70 (d, *J* = 5.2, 2H, Py H-2,6), 7.80 (d, *J* = 5.3, 2H, Py H-3,5), 2.20–1.96 (m, 1H, Cpr H-1), 1.17–0.69 (m, 4H, Cpr H-2,2′,3,3′); LC-MS: *m/z* = 265 [M+1], 266 [M+2]. Anal. calcd. for $C_{11}H_{12}N_4O_2S$: C, 49.99; H, 4.58; N, 21.20; S, 12.13. Found: C, 50.06; H, 4.63; N, 21.26; S, 12.16.

N-(2-Isonicotinoylhydrazine-1-carbonothioyl)benzamide (8)

Yield: 89.3%; mp 265–267 °C; IR (cm^{-1}): 1669, 1486, 1274, 1179, 756, 714, 668; ^{1}H NMR, δ, ppm (*J*, Hz): 12.59 (s, 1H, -C(O)NHC(S)-), 11.66 (s, 1H, -C(S)NHNHC(O)-), 11.34 (s, 1H, -C(S)NHNHC(O)-), 8.72 (d, *J* = 4.9, 2H, Py H-2,6), 8.05 (d, *J* = 7.5, 2H, Ph H-2,6), 7.84 (d, *J* = 4.9, 2H, Py H-3,5), 7.61 (t, *J* = 7.1, 1H, Ph H-4), 7.49 (t, *J* = 7.5, 2H, Ph H-3,5); LC-MS: *m/z* = 301 [M+1], 302 [M+2]. Anal. calcd. for $C_{14}H_{12}N_4O_2S$: C, 55.99; H, 4.03; N, 18.66; S, 10.67. Found: C, 56.05; H, 4.06; N, 18.72; S, 10.71.

N-(2-Carbamothioylhydrazine-1-carbonothioyl)-cyclopropanecarboxamide (9)

Yield: 60.3%; mp 252–254°C; IR (cm^{-1}): 3123, 1686, 1615, 1524, 1465, 1221, 1170, 1145, 943, 828, 734, 680, 639; ^{1}H NMR, δ, ppm (*J*, Hz): 13.37 (s, 1H, -C(O)NHC(S)-), 11.53 (s, 1H, -C(S)NHNHC(O)-), 10.49 (s, 1H, -C(S)NHNHC(O)-), 7.68 (s, 2H, NH_2), 2.05 (dt, *J* = 12.5, 6.3 Hz, 1H, Cpr H-1), 1.02–0.67 (m, 4H, Cpr H-2,2′,3,3′); ^{13}C NMR, δ, ppm: 182.05 (-C(O)NHC(S)-), 175.23 (-C(O)NHC(S)-), 169.59 (NHC(S)NH_2), 14.31 (Cpr C-1), 9.62 (Cpr C-2,3); LC-MS: *m/z* = 219 [M+1]. Anal. calcd. for $C_6H_{10}N_4OS_2$: C, 33.01; H, 4.62; N, 25.67; S, 29.37. Found: C, 33.17; H, 4.69; N, 25.72; S, 29.43.

4.2 | Antifungal activity

The mycelial growth rate assay was used for antifungal studies.[9] Strains of filamentous fungi were obtained from the following sources: *Asperillus niger* (AN) DSM 246, *Altenaria alternata* (AA) DSM 1102, *F. equiseti* (FE) DSM 21725, *F. graminearum* (FG) DSM 1095 and *F. fujikuroi* (FF) DSM 893, *Verticillium lecanii* (VL), *M. indicus* (MI) DSM 2185, *P. digitatum* (PD) DSM 2731 from DSMZ (Braunschweig, Germany); *Fusarium oxysporum* (FO) 39/1201 St. 9336 and *Botrytis cinerea* from the Technische Universität Berlin (Germany); *C. higginsianum* (CH) MAFF 305635, originally isolated in Japan, via the Department of Biology, Friedrich-Alexander-Universität (Erlangen, Germany). Oomycete strains *Phytophthora infestans* (PI GL-1) GL-1 01/14 wild strain, p-3 (PI p-3) (4/91; R+) and p-4 (PI p-4) (4/91; R−) were kindly donated by Julius Kühn-Institut (Quedlinburg, Germany). Potato dextrose agar (PDA) was purchased from C. Roth (Karlsruhe, Germany). Hymexazol (98%) was obtained from Prosperity World Store (Hebei, China). Strains were cultivated on PDA for 6 d at 25°C. Spores from each strain were gently harvested with a sterile glass rod from plate surfaces with deionized water. Spore concentration numbers in suspension were determined microscopically and adjusted to 7.5×10^6 spores/mL. Clear stock solutions of 5 mg/mL were made of 0.050 g of reference substance hymexazol or acyl thiourea in 10 mL of sterile dimethyl sulfoxide (DMSO). A total of 1 mL of each stock solution was mixed *in situ* into 99 mL of PDA prior to solidification to obtain a final concentration of 50 µg/mL. In the same way, series of PDA with tested compounds were prepared with final concentrations of 25, 10, 5, and 1 µg/mL. A total of 9 mL of each mixture were poured into 6 cm diameter petri dishes. After solidification central hole (diameter: 2.5 mm) was cut out and inoculated with 6.5 µL spore suspension. Plates were incubated at 25°C (±1°C) for 6 d. Control plates containing only PDA and water were prepared in the same way. Inhibitory effects (*I* %) were determined by analyzing growth zone diameters and calculated as described by Tang et al.[9]: $I\,\% = [(C - T)/(C - 2.5\ \text{mm})]) \times 100$, where *C* (mm) represents the growth zone of control PDA, and *T* (mm) is the average growth zone in the presence of reference or test substances. All growth experiments were carried out in triplicate. Means and standard deviations were calculated with software "Excel 2016" (Microsoft, USA).

4.3 | *Salmonella* reverse mutagenicity test

The mutagenicity test was applied as a standard plate incorporation assay with *Salmonella typhimurium* strains TA 98 and TA 100 as described by Maron and Ames.[10] Tested *Salmonella* strains were obtained from culture collection, University of Göteborg (Göteborg, Sweden). 2-Nitrofluorene (2-NF), dimethylsulfoxide (DMSO), 2-aminofluorene (2-AF), methyl methanesulfonate (MMS), β-nicotinamide adenine dinucleotide phosphate hydrate (β-NADP), and glucose-6-phosphate were purchased from Sigma–Aldrich (Steinheim, Germany), whereas D(+)-biotin, D(+)-glucose anhydrous, L-histidine and $NaNH_4HPO_4$ were sourced from Carl Roth GmbH & Co. KG (Karlsruhe, Germany). Citric acid monohydrate, NaCl, NaH_2PO_4, K_2HPO_4 anhydrous, $MgCl_2{}^*6H_2O$, KCl were purchased from Applichem GmbH (Darmstadt, Germany). NaOH solution was obtained from Riedel deHaen/Seelze (Hannover, Germany), $MgSO_4$ anhydrous was obtained from Merck (Darmstadt, Germany). Stock solutions of controls and acyl thioureas were solved in DMSO. Their final doses in top agar were adjusted to 50 and 500 µg/plate. The positive controls were 2-NF (10 mg/mL in DMSO; 10 µL/plate) for TA98 and methyl-methanesulfonate (MMS; 10 % (v/v) in DMSO; 1 µL/plate) for TA100; buffer with 100 µL of DMSO for both strains was used as negative control (i.e., determination of spontaneous reversion rate). In parallel experiments with metabolic activation were carried out by adding activated rat liver extract (S9-mix, Trinova Biochem, Giessen/Germany) instead of sodium buffer. Activity of S9-mix was confirmed with *Salmonella* TA 98 and 2-aminofluorene (2-AF, 10 mg/mL in DMSO, 10 µL/plate). All further experimental procedures were as described.[10]

4.4 | Frontier molecular orbitals calculations

All calculations based on semi-empirical molecular orbital theory have been carried out using ChemDraw 15.0[34] and HyperChem Professional 8.0[29] molecular modeling softwares. The structures of the investigated molecules in ground state were optimized using MM+ (molecular mechanics) and MNDO (modified neglect of the diatomic overlap) semi-empirical methods with RHF (restricted Hartree–Fock) basis. All calculations referred to the isolated molecule (gas phase). In this respect, the conjugate gradients algorithm (Polak-Ribier) was employed for the geometry optimization using a convergence set to the value of 0.01 kcal/(Å mol). The geometry optimization was done by minimization of the binding energy of the molecule. Based on theoretical MOs energy spectra the following molecular descriptors have been calculated: ionization potential (IP), electron affinity (EA), electronegativity (χ), chemical hardness (η) and softness (σ), and electrophilicity index (ω) according to the reported equations.[14,28]

4.5 | Molecular docking

Macromolecular data were downloaded from the Protein Data Bank (PDB),[35] namely, the crystal structures of sterol 14α-demethylase (CYP51) 5TZ1, topoisomerase II (Topo II) 1Q1D, L-glutamine:D-fructose-6-phosphate amidotransferase (GlcN-6-P) 1XFF, secreted aspartic proteinase (SAP2) 1EAG, *N*-myristoyltransferase (NMT) 1IYL, and UDP-*N*-acetylmuramoyl-L-alanine:D-glutamate ligase (MurD) 1UAG.

4.5.1 | Ligand preparation

Substances were drawn using MarvinSketch 17.21[36] and were saved in mol format. As reference hymexazol (3-hydroxy-5-methylisoxazol) was chosen.[9] Next, they were optimized by program Chem3D using molecular dynamics MM2 algorithm and saved as pdb-files. Molecular mechanics were used to produce more realistic geometry values for the majority of organic molecules owing to the fact of being highly parameterized. By using AutoDockTools-1.5.6 pdb-files were converted to PDBQT, and number of active torsions was set as default.[30]

4.5.2 | Protein preparation

PDB files were downloaded from the protein data bank.[35] Discovery Studio 4.0 was used to delete water molecules and ligand from the crystal. The proteins were saved as pdb-files. In AutoDockTools-1.5.6 polar hydrogens were added and saved as PDBQT. Grid box was set as follows: center_x = 70.728, center_y = 65.553, center_z = 3.865, size_x = 20, size_y = 20, size_z = 20. Vina was used to carry out docking. For visualization Biovia Discovery Studio Visualizer (v17.2.0.16349, Accelrys, San Diego, CA, USA) was applied.[37]

ACKNOWLEDGMENTS

Authors gratefully acknowledge "Enamine Ltd." (Kiev, Ukraine) and German Federal Ministry of Education and Research (Grant: FKZ 03FH025IX4) for financial support of this work; Federal Research Centre for Cultivated Plants (Quedlinburg, Germany) for presenting the strain *Phytophthora infestans*; Department of Biology, Friedrich Alexander University, Erlangen, Nürnberg, Germany for the strain *Colletotricum higginsianum*, and Dr. Oleksii Antypenko (Zaporizhzhya State Medical University, Ukraine) for conducting molecular docking.

CONFLICT OF INTEREST

The authors declare no competing financial interest.

ORCID

Lyudmyla Antypenko http://orcid.org/0000-0003-0057-1551
Sergiy Kovalenko http://orcid.org/0000-0001-8017-9108

REFERENCES

[1] M. C. Fisher, N. J. Hawkins, D. Sanglard, S. J. Gurr, *Science* **2018**, *360*, 739.
[2] A. Saeed, R. Qamar, T. A. Fattah, U. Flörke, M. F. Erben, *Res. Chem. Intermed.* **2017**, *43*, 3053.
[3] Thiourea. CASRN: 62-56-6. http://scorecard.goodguide.com/chemical-profiles/html/thiourea.html (25.06.2018).
[4] R. de O. Paiva, L. F. Kneipp, C. M. Goular, M. A. Albuquerque, A. Echevarria, *Ciencia e Agrotecnologia* **2014**, *38*, 531.
[5] A. Siwek, P. Staczek, A. Strzelczyk, J. Stefanska, *Lett. Drug Design Discov.* **2013**, *10*, 2.
[6] T. Kovač, M. Kovač, I. Strelec, A. Nevistić, M. Molnar, *Arh. Hig. Rada Toksikol.* **2017**, *68*, 9.
[7] K. G. Bedane, G. S. Singh, *ARKIVOC* **2015**, *6*, 206.
[8] J.-K. Wang, Y.-X. Zong, X.-C. Wang, Y.-L. Hu, G.-R. Yue, *CCL* **2015**, *26*, 1376.
[9] R. Tang, L. Jin, C. Mou, J. Yin, S. Bai, D. Hu, J. Wu, S. Yang, B. Song, *Chem. Cent. J.* **2013**, *7*, 1.
[10] D. M. Maron, B. N. Ames, *Mut. Res.* **1983**, *113*, 173.
[11] K. Mortelmans, E. Zeiger, *Mutat. Res. – Fundam. Mol. Mech. Mutagen.* **2000**, *455*(1–2), 29.
[12] G. F. Smith, *Prog. Med. Chem.* **2011**, *50*, 1.
[13] R. Benigni, A. Giuliani, R. Franke, A. Gruska, *Chem. Rev.* **2000**, *100*(10), 3697.
[14] J. A. H. Schwöbel, Y. K. Koleva, S. J. Enoch, F. Bajot, M. Hewitt, J. C. Madden, D. W. Roberts, T. W. Schultz, M. T. D. Cronin, *Chem. Rev.* **2011**, *111*(4), 2562.
[15] L. R. Domingo, M. Ríos-Gutiérrez, P. Pérez, *Molecules* **2016**, *21*(6), 748.
[16] Online SMILES Translator and Structure File Generator. NCI/CADD Group. https://cactus.nci.nih.gov/translate/ (06.05.2018).
[17] Molinspiration Cheminformatics Software, http://www.molinspiration.com/cgi-bin/properties (13.05. 2018).
[18] C. A. Lipinski, F. Lombardo, B. W. Dominy, P. J. Feeney, *Adv. Drug Delivery Rev.* **1997**, *23*, 3.
[19] D. F. Veber, S. R. Johnson, H. Y. Cheng, B. R. Smith, K. W. Ward, K. D. Kopple, *J. Med. Chem.* **2002**, *45*, 2615.
[20] P. B. Ertl, B. Rohde, P. Selzer, *J. Med. Chem.* **2000**, *43*, 3714.
[21] LogD Predictor. ChemAxon. Calculator Plugins. http://disco.chemaxon.com/apps/demos/logd/ (16.08. 2018).
[22] H. Pajouhesh, G. R. Lenz, *NeuroRx* **2005**, *2*(4), 541.
[23] S. A. Hitchcock, L. D. Pennington, *J. Med. Chem.* **2006**, *49*(26), 7559.
[24] J. B. Baell, G. A. Holloway, *J. Med. Chem.* **2010**, *53*(7), 2719.

[25] *Computational Toxicology Methods and Applications for Risk Assessment* (Ed: B. A. Fowler), ICF International, Fairfax, VA, USA **2013**.
[26] Bioactivity data associative promiscuity pattern learning engine, http://pasilla.health.unm.edu/tomcat/badapple/badapple (12.04. 2018).
[27] J. J. Yang, O. Ursu, C. A. Lipinski, L. A. Sklar, T. I. Oprea, C. G. Bologa, *J. Cheminform*. **2016**, *8*, 29.
[28] S. B. Gopalakrishnan, T. Kalaiarasi, R. J. Subramanian, *Comput. Meth. Phy*. **2014**, 1, Article ID 623235. https://doi.org/10.1155/2014/623235
[29] HyperChem release 7 for windows (user guide), USA. Hypercube, Inc., **2002**.
[30] O. Trott, A. J. Olson, *J. Comput. Chem*. **2010**, *31*, 455.
[31] R. L. Lopez de Compadre, A. K. Debnath, A. J. Shusterman, C. Hansch, *LUMO Environ. Mol. Mutagen*. **1990**, *15*(1), 44.
[32] V. André, C. Boissart, F. Sichel, P. Le Gauduchon, J. Y Talaër, J. C. Lancelot, C. Mercier, S. Chemtob, E. Raoult, A. Tallec, *Mutat. Res. – Genet. Toxicol. Environ. Mutagen*. **1997**, *389*(2–3), 247.
[33] T. Takamura-Enya, H. Suzuki, Y. Hisamatsu, *Mutagenesis* **2006**, *21*(6), 399.
[34] ChemDraw v15 User Guide, USA, PerkinElmer Informatics, Inc., **2015**.
[35] Worldwide Protein Data Bank. http://www.pdb.org (07.08. 2018).
[36] MarvinSketch version: 6.3.0, 2015, ChemAxon. http://www.chemaxon.com (07.08.2018).
[37] *PART V: Docking Strategies and Algorithms in Virtual Screening in Drug Discovery* (Eds: J. Alvarez, B. Shoichet), CRC Press, Taylor & Francis, Boca Raton, FL **2005**, Ch. 12.

SUPPORTING INFORMATION

Additional supporting information may be found online in the Supporting Information section at the end of the article.

How to cite this article: Antypenko L, Meyer F, Kholodniak O, et al. Novel acyl thiourea derivatives: Synthesis, antifungal activity, gene toxicity, drug-like and molecular docking screening. *Arch Pharm Chem Life Sci*. 2018;1–14. https://doi.org/10.1002/ardp.201800275